

# Measured Diameters of Two F-stars in the Beta Pic Moving Group

M. Simon<sup>1</sup> and G.H. Schaefer<sup>2</sup>

Received \_\_\_\_\_; accepted \_\_\_\_\_

---

<sup>1</sup>Department of Physics and Astronomy, Stony Brook University, Stony Brook, NY 11794  
michal.simon@stonybrook.edu

<sup>2</sup>The CHARA Array of Georgia State University, Mount Wilson Observatory, Mount Wilson, CA 91023, USA schaefer@chara-array.org

## ABSTRACT

We report angular diameters of HIP 560 and 21547, two F spectral type pre-main sequence members of the  $\beta$  Pic Moving Group. We used the East-West 314-m long baseline of the CHARA Array. The measured limb-darkened angular diameters of HIP 560 and 21547 are  $0.492 \pm 0.032$  and  $0.518 \pm 0.009$  mas, respectively. The corresponding stellar radii are 2.1 and 1.6  $R_{\odot}$  for HIP 560 and HIP 21547 respectively. These values indicate that the stars are truly young. Analyses using the evolutionary tracks calculated by Siess, Dufour, and Forestini and the tracks of the Yonsei-Yale group yield consistent results. Analyzing the measurements on an angular diameter *vs* color diagram we find that the ages of the two stars are indistinguishable; their average value is  $13 \pm 2$  MY. The masses of HIP 560 and 21547 are  $1.65 \pm 0.02$  and  $1.75 \pm 0.05$   $M_{\odot}$ , respectively. However, analysis of the stellar parameters on a Hertzsprung-Russell Diagram yields ages at least 5 MY older. Both stars are rapid rotators. The discrepancy between the two types of analyses has a natural explanation in gravitational darkening. Stellar oblateness, however, does not affect our measurements of angular diameters.

*Subject headings:* stars: Pre-Main Sequence— stars: Beta Pic Moving Group

## 1. Introduction

The age and mass of a pre-main sequence (PMS) star are usually estimated from its location in the Hertzsprung-Russell diagram (HRD) relative to theoretical calculations of stellar evolution. Unfortunately, differences among the theoretical calculations can produce mass and age estimates discrepant by factors of 2 to 3 (Hillenbrand and White, 2004; Simon, 2006). The consequences are that the mass-spectrum of stars produced in a star-forming region, the region’s star-forming history, and the chronology of planet formation are imprecisely known. The latter point has taken on a pressing importance as astronomers are poised to detect exoplanets associated with young stars.

Measurement of the diameters of young stars as they contract to the main sequence can provide their ages and a new independent test of the theoretical PMS evolutionary tracks (Simon, 2006). Once a reliable set of evolutionary tracks is established, measurement of the diameters of PMS stars will yield measurements of their absolute ages. Remarkably, members of the  $\beta$  Pic Moving Group (BPMG) are young enough (10-20 MY) and near enough ( $< 50$  pc; e.g. Torres et al., 2006) that some are resolvable with the optical/IR interferometric array of the Center for High Angular Resolution Astronomy (CHARA). The brighter members of the BPMG have parallaxes measured by *HIPPARCOS*. The ages of individual stars in the BPMG are determined by HRD fitting and the strength of the Li-line. An age for the group as a whole may be estimated dynamically by tracing the group’s motion back to a common origin. The age estimates range from  $11.2 \pm 0.3$  to  $22 \pm 12$  MY (see Table 2 in Fernadez et al. 2008; Yee and Jensen, 2010). Whether the spread represents uncertainties of the dating methods or a range in individual formation times is unknown. Astronomers already have evidence of planet formation associated with the members of the BPMG. Lagrange et al (2010) imaged the exoplanet of  $\beta$  Pic, an A-star. Debris disks are understood as indicators of planet formation (Quillen et al. 2007);  $\beta$  Pic

and AU Mic, a BPMG member of M1 spectral type, are known to have debris disks (Smith and Terrile 1984; Lagrange et al 2010; Liu 2004).

We measured the angular diameters of two stars in the BPMG , HIP 560 and 21547, using the CHARA Array. §2 describes our observations and §3 presents our analysis and discussion of the diameter measurements. We summarize our results in §4.

## 2. Interferometric Measurements of HIP 560 and HIP 21547

We observed at the CHARA Array located on Mt. Wilson, CA, on the nights of UT 11, 12, and 13 Sept. 2010. Our observing assignment was made through an allotment made available competitively to the astronomical community by CHARA and administered by the National Optical Astronomical Observatory through its observing time application process. The array consists of six 1-m telescopes in a Y-configuration on baselines from 34 to 331 m (ten Brummelaar et al. 2005). We used the CLASSIC beam combiner operating in the H and K' bands to observe with the two telescopes on the 314 m E1-W1 baseline. At the CHARA Array these bands are centered at 1.673 and 2.133  $\mu m$  wavelengths, with bandwidths, 0.285 and 0.349  $\mu m$  respectively.

Table 1 lists the properties of HIP 560 and HIP 21547 we need for this paper; the parallactic distances are van Leeuwen et al.'s (1997) revised *HIPPARCOS* values. Neither star is known to be a spectroscopic binary. HIP 21547 is one component of a common proper motion binary; its companion, GJ 3305, is at about  $1'$  angular separation. We checked the near-IR and thermal-IR fluxes of the stars as given by *2MASS* and *WISE*<sup>1</sup>. Neither shows evidence of excess emission in the near-IR. HIP 560 is not included in the *WISE* Preliminary Data Release. For HIP 21547, the *WISE* magnitudes at 3.6, 12, and 22

---

<sup>1</sup><http://irsa.ipac.caltech.edu>

$\mu\text{m}$  are consistent with the *2MASS* K-band magnitude,  $\sim 4.5$  (Table 1). HIP 21547 is  $\sim 0.5$  mag brighter in *WISE* band 2 at  $4.5 \mu\text{m}$ ; on a color-color diagram this still places the star in the region of normal stars without a debris disk. Both stars are rapid rotators with values of  $v \sin i$  in the range typical of F stars (Abt and Hunter 1962).

The essential observational datum of an interferometer measurement is the fringe contrast or visibility,  $V$ , of the target or calibrator. An observation of a program star or its calibrators took about 10 minutes each and consisted of a series of data scans through the central interferometer fringe and a sequence of shutters. Each program star observation was bracketed by observations of one or two stellar calibrators with angular diameters smaller than  $0.3 \text{ mas}$  and located within  $10^\circ$  of the target (Table 1). An observation of HIP 560 or 21547 and their calibrators required about 2 hours to obtain good S/N.

The calibrators were chosen to be unresolved by the interferometer, but their diameters are nonetheless finite (Table 1). S. Ridgway (priv. comm.) kindly estimated the limb-darkened diameters,  $\phi_{LD}$ , of the calibrators, using Kervella et al’s (2004) angular diameter fits for main sequence stars as a function of their V-K color, K-band magnitude, the parallactic distance of the star, and an estimate of its extinction (always small,  $A_V \leq 0.07$ ). We scaled the observed calibrator visibilities to those of a point-like star. We then calibrated the target visibilities by ratioing them to the scaled calibrator visibilities. Table 2 lists the wavelength, MJD time of observation, projected baseline in meters, its position angle on the sky, measured eastward from north, the calibrated visibilities  $V_{cal}$  of the targets, and their uncertainties  $\sigma_{Vcal}$ . The  $\sigma_{Vcal}$  include the uncertainties of the measured visibilities of target and calibrators and an assumed  $\pm 10\%$  uncertainty in the calculated diameters of the calibrators.

Figures 1 and 2 show the calibrated visibilities at H and K *vs* spatial frequency (projected baseline/wavelength). Fig. 1 for HIP 560 indicates a systematic difference in

angular diameters measured at H and K. We do not think this can be attributed to a property of the star because HIP 21547, also an F spectral type star, does not show the effect. The difference is probably measurement error. At angular diameters as small as those of HIP 560 and HIP 21547 the curves for a uniform disk and limb-darkened disk are nearly indistinguishable<sup>2</sup>. Nonetheless, we did analyze the visibilities with respect to limb-darkened models following Hanbury-Brown et al.’s (1974) analysis. Their expression for the visibility of a limb-darkened star can be written

$$V_{LD}(x) = [\frac{1 - u_\lambda}{2} + \frac{u_\lambda}{3}]^{-1} [\frac{1}{2}(1 - u_\lambda)V_{UD} + \frac{u_\lambda}{x^2}(\frac{\sin x}{x} - \cos x)]$$

where  $V_{UD}$  is the visibility of a uniform stellar disk,  $V_{UD} = 2\frac{J_1(x)}{x}$ , in which  $J_1$  is the Bessel function of order 1, and  $x = \frac{\pi\phi B}{\lambda}$  with  $\phi$  the star’s angular diameter,  $B$  the projected baseline during the scan, and  $\lambda$  the wavelength of observation. We used values of the limb darkening parameter,  $u_\lambda$ , derived by Claret et al (1995) appropriate to stars that have effective temperatures of 1.5 to 1.7  $M_\odot$  stars 10 to 20 MY old,  $u_\lambda = 0.24$  and 0.20, at H and K respectively. We included a  $\pm 10\%$  uncertainty in the values of  $u_\lambda$  in the calculation of the uncertainties of the measured stellar diameters.

We fit each calibrated visibility to a limb-darkened diameter, averaged the individual values, and present the results,  $\overline{\phi_{Diam}(mas)}$ , for HIP 560 and 21547 in Table 3. The uncertainties are standard deviations of the mean. The uncertainties are dominated by the scatter of the individual visibility measurements. Table 3 also lists  $\overline{\Phi_{Diam}}$  the “absolute” angular diameter, the value of  $\phi$  scaled to a common distance of 10 pc and the corresponding stellar radii. The uncertainties in  $\overline{\Phi_{Diam}}$  include the uncertainties in the HIPPARCOS

---

<sup>2</sup>This would not be true for stars more strongly limb-darkened than F-stars (van Belle et al. 2001).

distances (van Leeuwen et al. 2007).

### 3. Analysis and Discussion

#### 3.1. Analysis in the $\Phi$ vs $(V - K)$ and the HR Diagrams

Figure 3 shows  $\overline{\Phi_{Diam}}$  compared with diameters predicted by PMS evolution models calculated by Siess et al (2000) (SDF) and the Yonsei-Yale (Y2) models calculated by Yi et al (2003). The Y2 calculations<sup>3</sup> provide the luminosity,  $L$ , and effective temperature,  $T_{eff}$  at 5 MY intervals during the contraction; we calculated the corresponding radii through the defining relation  $L = 4\pi R^2 \sigma T_{eff}^4$  where  $\sigma$  is the Stefan-Boltzmann constant. The SDF website provides the photospheric radii directly<sup>4</sup> and connects  $T_{eff}$  to magnitudes using Kenyon and Hartmann’s (1995) Table A5. To present the Y2 results with  $(V - K)$  as the independent variable, we interpolated their  $T_{eff}$  to the Kenyon and Hartmann scale. The diameter measurements indicate, for both stars, ages in the range 10-15 MY and masses 1.6 to 1.8  $M_{\odot}$ . The left-hand portion of Table 3 lists more precise values obtained by placing the observed diameters on a finer mesh in the  $\Phi$  vs  $(V - K)$  color diagram (henceforth the  $\Phi CD$ ); the values lie in the columns designated  $\Phi_{SDF}$  and  $\Phi_{Y2}$ . The age difference between HIP 560 and 21547 is not statistically significant and the SDF and Y2 tracks yield values that are in good agreement. The average age of the two stars is  $13 \pm 2$  MY. The masses determined using the SDF and Y2 tracks are also consistent. The average mass of HIP 560 is  $1.65 \pm 0.02 M_{\odot}$  and that of HIP 21547,  $1.75 \pm 0.05 M_{\odot}$ .

If we did not have angular diameter measurement of HIP 560 and 21547, the only way to estimate their age and mass would be by their positions on an HRD relative theoretical

---

<sup>3</sup>[www.astro.yale.edu/demarque/yystar.html](http://www.astro.yale.edu/demarque/yystar.html)

<sup>4</sup>[www-astro.ulb.ac.be/~siess/](http://www-astro.ulb.ac.be/~siess/)

isochrones. Figure 4 shows such an analysis, here on an HRD plotted as  $M_K$  vs  $(V - K)$ . It is seen that both the SDF and Y2 tracks indicate ages at least 5 MY older, and masses  $\sim 0.2 M_\odot$  smaller than those indicated by the  $\Phi CD$  (the columns designated  $HRD_{SDF}$  and  $HRD_{Y2}$  in Table 4).

The observational inputs, angular diameters, distances, and photometry, and hence the stellar radii, luminosities, and effective temperatures give essentially the same ages and masses whether the SDF or Y2 models are used. The results are however consistently discrepant when interpreted on the  $\Phi CD$  or the HRD. This suggests that the source of the discrepancy lies in the application of theoretical calculations of non-rotating stars to stars that rotate with high angular velocities.

### 3.2. The Effects of Stellar Rotation

The rotation of stars less massive than  $\sim 2 M_\odot$  slows over their lifetimes because stellar winds powered by the convective outer layers carry away their angular momentum. The convective zone in main-sequence F spectral type stars disappears toward the earlier F spectral type sub-classes and energy transport becomes entirely radiative. This explains the rapid decrease of  $v \sin i$  from F0V to F9V (e.g. Abt and Hunter 1962; Kraft 1967). The observation and theoretical analysis of stellar rotation have a rich history (e.g. Tassoul 2000) and its effects are revealed beautifully now that stars can be imaged interferometrically (e.g. Peterson et al. 2006 a,b; Monnier et al. 2007; Zhao et al. 2009; Che et al. 2011).

The effective surface gravity,  $g_{eff}$  in a rotating star decreases from the pole to the equator. This produces oblateness and a brightness variation with latitude known as gravity darkening. The oblateness of a rotating star in radiative equilibrium is given by



$$o = \frac{R_e - R_p}{R_e} = 0.77 \frac{\omega^2}{2\pi G \rho_m}$$

where  $R_e$  and  $R_p$  are the equatorial and polar radii,  $\omega$  is the angular velocity, and  $\rho_m$  is the mean density (von Zeipel 1924; Chandrasekhar 1933). Inserting numerical values,

$$o = 0.0261 \left( \frac{R_p}{R_\odot} \right) \left( \frac{M_\odot}{M_*} \right) \left( \frac{V_{eq}}{100 \text{ km/s}} \right)^2$$

where  $R_p$  is the polar radius of the star, and  $M_*$  and  $V_{eq}$  are its mass and equatorial velocity. Sackmann (1970) showed that the decrease of  $R_p$  from its non-rotating value is only a few percent even when the star is rotating nearly at break-up. At break-up,  $R_{eq} = 3/2 R_p$ ,  $o = 0.33$  and  $V_{eq,bk}^2 = 2GM_*/3R_p$  (eg Collins, 1963). It is safe to apply these results to HIP 560 and 21547 because Demarque and Roeder (1967) showed that the outer convective layers disappear at F early spectral type.

To make numerical estimates of the expected oblateness for HIP 560 and 21547, we use values from SDF for the radius and mass of an early F spectral type star at age 13MY,  $R_* = 1.7R_\odot$ ,  $M_* = 1.7M_\odot$ . We use these values because, in principle, our measured values could be affected by oblateness. We also use the  $v \sin i$  values, 171 and 95 km/s, measured for HIP 560 and 21547, respectively (Table 1). Since the inclinations are not known we cannot calculate the equatorial velocities. We can, however, estimate them by calculating the expectation values  $\langle v \sin i \rangle$ . The upper bound on the inclination is  $i = \pi/2$ . If the lower bound on  $i$  were 0,  $\langle v \sin i \rangle = V_{eq}\pi/4$ . Here, however, a lower bound,  $i_{crit}$ , is set by the value at which  $v \sin i_{crit}$  would imply rotation at the breakup velocity. For the adopted radius and mass,  $V_{eq,bk} = 357$  km/s. Hence,  $\sin i_{crit} = (\text{observed } v \sin i)/357$  and  $i_{crit} = 8.6^\circ$  and  $15.4^\circ$  for HIP 560 and 21547 respectively. Using these values as a lower bound on the inclination, the expectation values of the equatorial velocities are 202 and 118 km/s, and of the oblateness, 0.104 and 0.036, for HIP 560 and 21547 respectively. These values

could be measured only if the stars’ rotation axes were positioned for best resolution of the oblateness with the east-west baseline of the CHARA array. The measured oblateness values are therefore likely to be smaller. In the case of HIP 21547 our observations probably would not have measured  $o \leq 0.036$  because the precision of the diameter measurement is  $\sim 2\%$  (Table 3). For HIP 560, in the unlikely case that a  $\sim 10\%$  oblateness accounts for the measured value of its angular diameter, a 10% smaller value of  $\Phi$  would still place it between the 10 and 20 MY isochrones. We conclude that stellar oblateness probably does not enter into the interpretation of our results<sup>5</sup>.

In a rotating star in radiative equilibrium, the radiative flux at a point on the photosphere is proportional to  $g_{eff}$  (von Zeipel 1924). Since  $g_{eff}$  decreases from the pole to the equator, the corresponding decrease in radiative flux can be characterized as a decrease in the local effective temperature and is called gravity darkening. In the A spectral type stars that have been imaged (Peterson et al. 2006a,b; Monnier et al. 2007; Zhao et al. 2009), the temperature difference is large,  $\sim 2000\text{K}$ . Thus, relative to a non-rotating star, a rotating star seen pole-on ( $i = 0$ ) will appear brighter and its photometric color will be hotter than one seen equator-on ( $i = \pi/2$ ). Observed values for a given star depend, of course, on its inclination. Maeder and Peytremann (1970) have calculated the photometric effects for stars of mass 1.4, 2, and 5  $M_{\odot}$  at various values of  $V_{eq}$  and  $i$ . Typically the values of  $M_V$  vary by a few tenths mag and of  $(B - V)$  by a few hundredths. Details depend on the stellar mass and inclination; Maeder and Peytremann’s calculations show that for  $i \gtrsim 54^\circ$  the rotating star appears less bright and redder than a non-rotating star.

The effects of gravity darkening suggest that the discrepancies summarized in Table 4 are attributable to rotation of HIP 560 and 21547. If their rotational velocities and

---

<sup>5</sup>Also, the on-sky angle of the projected baseline was essentially the same throughout our observations (Table 2). Thus baseline rotation during our observations is not an issue.

inclinations are such that their absolute magnitudes at K are depressed by a few tenths relative to a non-rotating star and their  $(V - K)$  are slightly redder, the ages and masses deduced from the  $\Phi CD$  and HRD could be in agreement. A detailed test of this hypothesis will be possible when the inclinations of these stars are measured. This can be accomplished by either measuring their light fluctuations and thus rotational periods or by interferometric imaging of their photospheric emission of these stars is mapped. The first approach is possible now as Garcia-Alvarez et al. (2011) demonstrated by measuring the periods and inclinations of two other stars in the BPMG.

### 3.3. Implications for the BPMG

If we accept the results of the  $\Phi CD$  analysis and attribute the discrepancy of results from the HRD to stellar rotation, we conclude that HIP 560 and 21547 are roughly coeval at an average age of about 13 MY. Their galactic (X,Y,Z) coordinates (Table 1) place them about 49 pc apart with each moving at speed  $\sim 22$  km/s given by their (U,V,W) velocity components. It is too soon to attribute the results for this pair to all the stars in the BPMG but our results suggest that the members were born together about 13 MY ago, and thus are at the younger end of the age span described in §2.

## 4. Summary and Future Directions

- 1) The measured angular diameters of HIP 560 and HIP 21547 in the H and K bands are  $0.492 \pm 0.032$  and  $0.518 \pm 0.009$  mas, respectively. Scaled to a common distance 10pc, their angular diameters are  $\Phi = 1.94 \pm 0.13$  and  $1.52 \pm 0.03$  mas.
- 2) Analyzing these results in  $\Phi$  vs  $(V - K)$  diagram with SDF and Y2 isochrones calculated yields ages of the two stars that are not different at a statistically significant level. Their

average age is  $13 \pm 2$  MY. The masses determined according to the two sets of isochrones also do not differ at a statistically different level. The average values are  $1.65 \pm 0.02 M_{\odot}$  for HIP 560 and  $1.75 \pm 0.05 M_{\odot}$  for HIP 21547.

3) Analyzing the stellar parameters with the SDF and Y2 isochrones in a conventional HR diagram yields ages at least 5 MY older and masses  $\sim 0.2 M_{\odot}$  smaller.

4) HIP 560 and 21547 are rapid rotators (Table 1). The discrepancy in ages and masses can be accounted for by gravitational darkening of rotating stars in radiative equilibrium. A detailed test of this hypothesis will be possible when their inclinations are determined either by measuring their rotational periods or by interferometric images of their photospheres.

5) Taken together, our results suggest that HIP 560 and 21547 formed coevally about 13 MY ago.

The most pressing task is to determine whether the 13 MY age applies to the BPMG as a whole. Although most BPMG are in the southern hemisphere, at least 3 other F and G spectral type stars are bright and near enough for measurement with the CHARA array. Stars of later spectral type are too faint for observation at the present time unless, by good luck, they are close to the sun. Many more of the BPMG members will be observable when the planned sensitivity improvements at the CHARA array are realized.

We thank the referee for a helpful and unusually warm report. We are grateful to Steve Ridgway for advice and help with the observations. We thank Deane Peterson for reminding us that F-stars can rotate rapidly, for advice about stellar rotation, and for pointing out the Garcia-Alvarez paper. We thank the CHARA staff at Mt. Wilson for thorough support. The CHARA Array is operated by Georgia State University's Center for High Angular Resolution Astronomy on Mount Wilson, California. Access to the CHARA

Array, which is operated with funding from the National Science Foundation and Georgia State University, was obtained through a competitive TAC process administered by the National Optical Astronomy Observatory. Our work was supported in part by NSF Grant AST-09-08406. We used data products from the Two Micron All Sky Survey, which is a joint project of the University of Massachusetts and the Infrared Processing and Analysis Center/California Institute of Technology, funded by the National Aeronautics and Space Administration and the National Science Foundation. Our research has also used of the SIMBAD database operated at CDS, Strasbourg, France.

## References

- Abt, H.A. and Hunter, J.H., Jr., 1962, ApJ, 136, 381
- Chandrasekhar, s., 1933, MNRAS, 93, 390
- Che, X. et al. 2011 ApJ, 732, 68
- Claret, A., Diaz-Cordoves, J., and Gimenez, A. 1995, A&AS, 114, 247
- Collins, G.W. 1963, ApJ, 138, 1134
- Demarque, P. and Roeder, R. 1967 ApJ, 147, 1188
- Fernandez, D., Figueras, F., & Torra, J. 2008, A&A, 480, 735
- Garcia-Alvarez, D. et al. , 2011, arXiv:1107.5688v2
- Hanbury-Brown, R., Davis, J., Lake, R.J.W., and Thompson, R.J. 1974, MNRAS, 167, 475
- Hillenbrand, L. and White, R. 2004, ApJ604, 741
- Kenyon, S. J., & Hartmann, L. 1995, ApJS, 101, 117
- Kervella, P. et al. 2004, A&A, 426, 297
- Kraft, R. 1967, ApJ, 150, 551
- Lagrange, A.-M. et al. 2010, Science, 329, 57
- Liu, M. 2004, Science, 305, 1442
- Maeder, A. and Peytremann,E 1970, A&A, 7, 120
- Monnier, J.D. et al. 2007, Science, 317, 342
- Peterson, D.M. 2006a, Nature, 440, 896
- Peterson, D.M. 2006b ApJ, 636, 1087

- Quillen, A.C., Morbidelli, A. and Moore, A. 2007 MNRAS, 380, 1642
- Sackmann, I.-J. 1970 A&A, 8, 76
- Siess, L., Dufour, E. & Forestini, M. 2000, A&A, 358, 593 (SDF)
- Simon, M. 2006 in *The Power of Optical/IR Interferometry*, (Springer: Berlin), A. Richichi, F. Delplancke, F. Paresce, & A. Chelli, eds, p. 227
- Smith, B.A. and Terrile, R.J. 1984, 226, 1421
- Tassoul, J.-L. 2000 *Stellar Rotation* (Cambridge University Press: Cambridge)
- ten Brummelaar, T. A., et al. 2005, ApJ, 628, 453
- Torres, C. A. O., Quast, G. R., da Silva, L., de La Reza, R., Melo, C. H. F., Sterzik, M. 2006, A&A, 460, 695
- van Belle, G. et al. 2001, ApJ, 559, 1155
- van Leeuwen, F. et al. 1997, A&A, 323, L61
- von Zeipel, H. 1924, MNRAS, 84, 684
- Yee, J.C. and Jensen, E.L.N. 2010, ApJ, 711, 303
- Yi,S., Kim, Y.-C., and Demarque, P. 2003 ApJS, 144, 259
- Zhao, M. et al. 2009 ApJ, 701, 209

Table 1. Properties of HIP 560 and HIP 21547

	HIP 560	HIP 21547
Alternate Name	HD 203	HD 29391
Spectral Type	F3V	F0V
V(mag)	6.19	5.22
K(mag)	5.24	4.54
$v \sin i$ (km/s)	170.7	95.0
Distance (pc)	$39.4 \pm 0.4$	$29.4 \pm 0.3$
X,Y,Z (pc)	4.5, 5.8, -38.4	-24.3, -8.2, -15.2
U,V,W (km/s)	-10.4, -14.5, -13.3	-14.0, -16.2, -10.1
Calibrators:		
	HD 268	HD 26794
$\phi_{LD}$ (mas)	0.27	0.25
	HD 223884	
$\phi_{LD}$ (mas)	0.26	
Data for $\beta$ Pic targets from Torres et al. (2006)		



Table 2. Calibrated Visibilities

Object	$\lambda$	MJD	$B$ (m)	PA ( $^\circ$ )	$V_{cal}$	$\sigma_{V_{cal}}$
HIP 560	K	55450.286	308.62	69.69	0.828	0.018
HIP 560	K	55450.300	311.91	71.87	0.783	0.016
HIP 560	K	55450.314	313.44	73.94	0.751	0.015
HIP 560	K	55450.332	312.66	76.38	0.866	0.017
HIP 560	K	55450.347	309.38	78.47	0.863	0.016
HIP 560	K	55452.314	313.51	74.74	0.839	0.015
HIP 560	K	55452.324	312.91	76.10	0.814	0.015
HIP 560	K	55452.334	311.39	77.39	0.856	0.015
HIP 560	H	55451.328	312.81	76.22	0.853	0.028
HIP 560	H	55451.342	310.18	78.08	0.897	0.025
HIP 560	H	55451.355	305.80	79.82	0.893	0.025
HIP 560	H	55451.370	298.79	81.72	0.866	0.026
HIP 21547	K	55450.515	313.26	75.68	0.849	0.013
HIP 21547	K	55450.525	313.44	75.86	0.819	0.012
HIP 21547	K	55450.535	312.45	75.96	0.860	0.014
HIP 21547	H	55451.501	311.41	75.40	0.769	0.021
HIP 21547	H	55451.515	313.41	75.73	0.776	0.022
HIP 21547	H	55451.533	312.20	75.97	0.766	0.021
HIP 21547	H	55451.544	310.15	76.02	0.775	0.021
HIP 21547	H	55452.496	311.11	75.37	0.773	0.022
HIP 21547	H	55452.513	313.43	75.73	0.719	0.020
HIP 21547	H	55452.521	313.31	75.88	0.791	0.022
HIP 21547	H	55452.533	311.69	75.99	0.729	0.020

Table 3. Measured Sizes

	HIP 560	HIP 21547
$\overline{\phi(mas)}$	$0.492 \pm 0.032$	$0.518 \pm 0.009$
$\overline{\Phi(mas)}$	$1.94 \pm 0.13$	$1.52 \pm 0.03$
$R/R_\odot$	$2.08 \pm 0.14$	$1.63 \pm 0.03$

Table 4. Measured Ages and Masses

Star	$\Phi_{SDF}$	$\Phi_{Y2}$	HRD <sub>SDF</sub>	HRD <sub>Y2</sub>
Age (MY)				
HIP 560	$12.0 \pm 3.0$	$10 \pm 2$	$25^{+25}_{-8}$	$18 \pm 2$
HIP 21547	$15.0 \pm 2.0$	$15 \pm 2$	$20^{+30}_{-2}$	$18 \pm 2$
Mass ( $M_{\odot}$ )				
HIP 560	$1.68 \pm 0.03$	$1.63 \pm 0.02$	$1.49 \pm 0.05$	$1.45 \pm 0.10$
HIP 21547	$1.75 \pm 0.05$	$1.75 \pm 0.05$	$1.56 \pm 0.05$	$1.55 \pm 0.10$

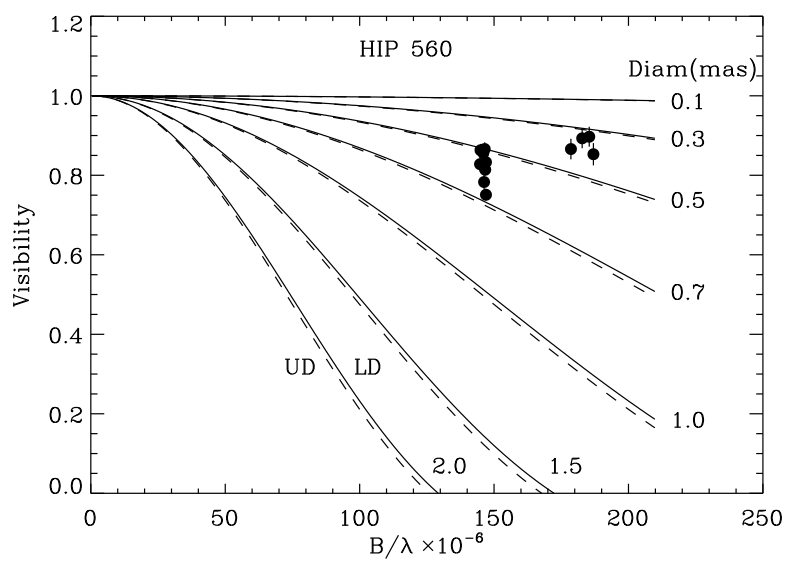


Fig. 1.— Calibrated visibilities of HIP 560 at H and K *vs* spatial frequency, the projected baseline divided by the wavelength. The dashed curves are for uniform disk models (UD) with the diameters indicated and the solid curves are limb-darkened models.

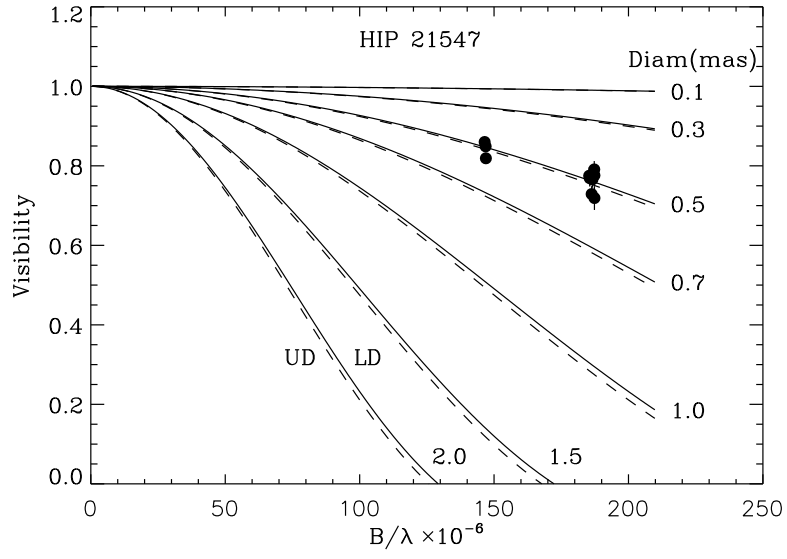


Fig. 2.— Same as Fig. 1 but for HIP 21547.

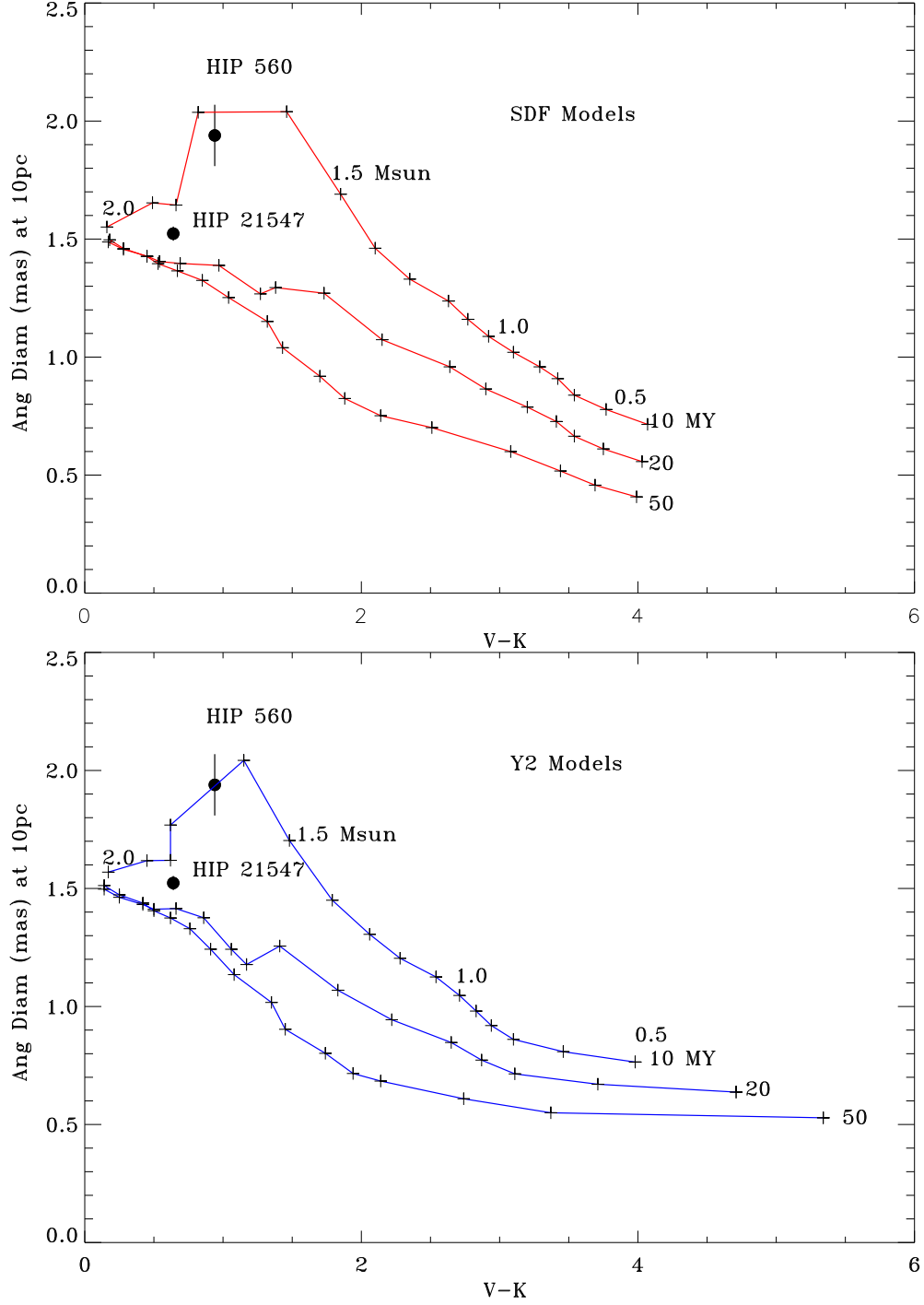


Fig. 3.— HIP 560 and 21547 angular diameters scaled to 10pc distance *vs* (V-K) compared to isochrones at 10, 20, and 50 MY calculated by SDF (top) and Y2 (bottom). The crosses indicate masses 0.4 to 2.0  $M_{\odot}$  at 0.1  $M_{\odot}$  intervals for the SDF isochrones and 0.5 to 2.0  $M_{\odot}$  for the Y2 isochrones.

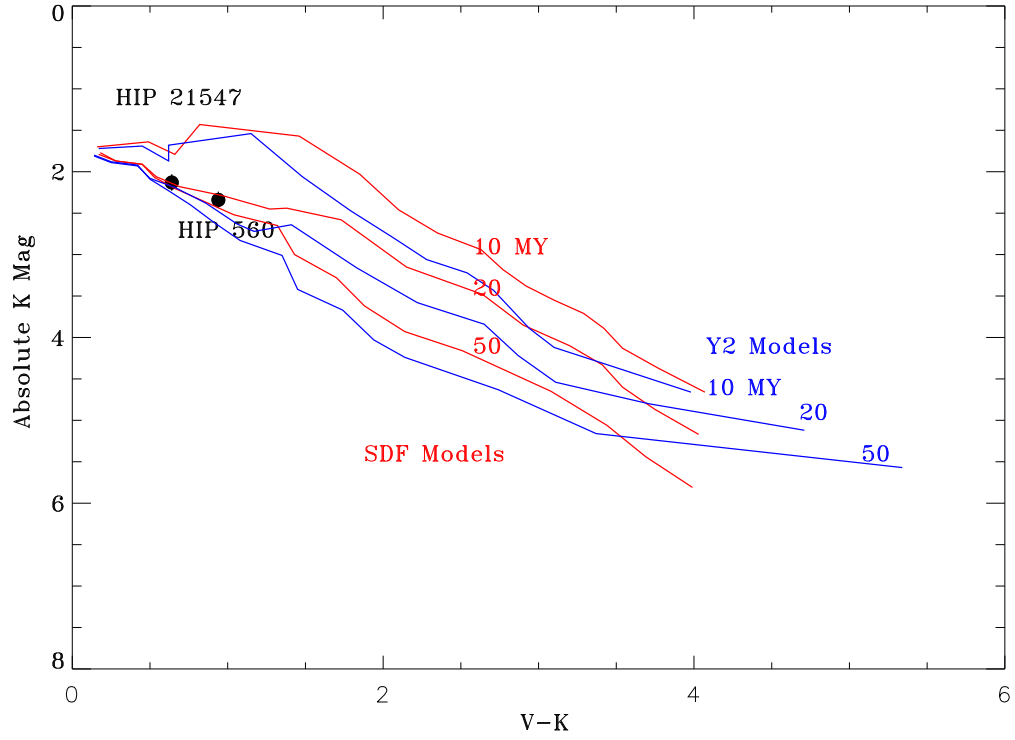


Fig. 4.— HIP 560 and 21547 on a conventional Hertzsprung-Russell diagram here presented as  $M_K$  vs (V-K). The isochrones are calculated by SDS and Y2 as in Fig. 3.